TU/e EINDHOVEN UNIVERSITY OF TECHNOLOGY

Understanding the catalytic activity of single-chain polymeric nanoparticles in water

Citation for published version (APA):
Artar, M., Terashima, T., Sawamoto, M., Meijer, E. W., & Palmans, A. R. A. (2014). Understanding the catalytic activity of single-chain polymeric nanoparticles in water. *Journal of Polymer Science, Part A: Polymer Chemistry*, *52*(1), 12-20. https://doi.org/10.1002/pola.26970

DOI:
10.1002/pola.26970

Document status and date:
Published: 01/01/2014

Document Version:
Publisher's PDF, also known as Version of Record (includes final page, issue and volume numbers)

Please check the document version of this publication:

• A submitted manuscript is the version of the article upon submission and before peer-review. There can be important differences between the submitted version and the official published version of record. People interested in the research are advised to contact the author for the final version of the publication, or visit the DOI to the publisher's website.
• The final author version and the galley proof are versions of the publication after peer review.
• The final published version features the final layout of the paper including the volume, issue and page numbers.

Link to publication

General rights
Copyright and moral rights for the publications made accessible in the public portal are retained by the authors and/or other copyright owners and it is a condition of accessing publications that users recognise and abide by the legal requirements associated with these rights.

• Users may download and print one copy of any publication from the public portal for the purpose of private study or research.
• You may not further distribute the material or use it for any profit-making activity or commercial gain
• You may freely distribute the URL identifying the publication in the public portal.

If the publication is distributed under the terms of Article 25fa of the Dutch Copyright Act, indicated by the "Taverne" license above, please follow below link for the End User Agreement:

www.tue.nl/taverne

Take down policy
If you believe that this document breaches copyright please contact us at:

openaccess@tue.nl

providing details and we will investigate your claim.

Download date: 23. Aug. 2022

Understanding the Catalytic Activity of Single-Chain Polymeric Nanoparticles in Water

Müge Artar,[1,2] Takaya Terashima,[3] Mitsuo Sawamoto,[3] E. W. Meijer,[1,2] Anja R. A. Palmans[1,2]

[1]Institute for Complex Molecular Systems, Eindhoven University of Technology, PO Box 513, 5600 MB Eindhoven, The Netherlands
[2]Laboratory of Macromolecular and Organic Chemistry, Eindhoven University of Technology, PO Box 513, 5600 MB Eindhoven, The Netherlands
[3]Department of Polymer Chemistry, Graduate School of Engineering, Kyoto University, Katsura, Nishikyo-ku, Kyoto 615–8510, Japan
Correspondence to: T. Terashima (E-mail: terashima@living.polym.kyoto-u.ac.jp) or E. W. Meijer (E-mail: e.w.meijer@tue.nl) or A. R. A. Palmans (E-mail: a.palmans@tue.nl)

Received 29 August 2013; accepted 1 October 2013; published online 24 October 2013
DOI: 10.1002/pola.26970

ABSTRACT: The structuring role of benzene-1,3,5-tricarboxamide (BTA) groups for the catalytic activity of single chain polymeric nanoparticles in water was investigated in the transfer hydrogenation of ketones. To this end, a set of segmented, amphiphilic copolymers was prepared, which comprised oligo (ethylene glycol) side chains to impart water solubility, BTA and/or lauryl side chains to induce hydrophobicity and diphenylphosphinostyrene (SDP) units in the middle part as a ligand to bind a ruthenium catalyst. All copolymers were obtained by reversible addition-fragmentation chain transfer (RAFT) polymerization and showed low dispersities ($M_w/M_n = 1.23$–1.38) and controlled molecular weights ($M_n = 44$–28 kDa). A combination of circular dichroism (CD) spectroscopy and dynamic light scattering (DLS) showed that all copolymers fold into a single chain polymeric nanoparticles (SCPNs) as a result of the helical self-assembly of the pendant BTA units and/or hydrophilic–hydrophobic phase separation. To create catalytic sites, $RuCl_2(PPh_3)_3$ was incorporated into the copolymers. The Cotton effects of the copolymers before and after Ru(II) loading were identical, indicating that the helical self-assembly of the BTA units and the complexation of SDP ligands and Ru(II) occurs in an orthogonal manner. DLS revealed that after Ru(II) loading, SDP-bearing copolymers retained their single chain character in water, while copolymers lacking SDP units clustered into larger aggregates. The Ru(II) loaded SCPNs were tested in the transfer hydrogenation of cyclohexanone. This study reveals that BTA induced stack formation is not crucial for SCPN formation and catalytic activity; SDP-bearing copolymers folded by Ru(II) complexation and hydrophobic pendants suffice to provide hydrophobic, isolated reaction pockets around Ru(II) complexes. © 2013 Wiley Periodicals, Inc. J. Polym. Sci., Part A: Polym. Chem. **2014**, *52*, 12–20

KEYWORDS: benzene-1,3,5-tricarboxamide (BTA); catalysis; reversible addition-fragmentation chain transfer (RAFT) polymerization; ruthenium; transfer hydrogenation

INTRODUCTION Enzymes are highly attractive for performing reactions in water on an industrial scale and a source of inspiration to design novel catalytic systems. On the other hand, creating sufficiently hydrophobic domains around the catalytic sites to ensure compatibility of the homogeneous organo- or metal-based catalysts with aqueous environments has remained a major challenge.[1–3] For this reason, artificial metalloenzymes,[4–6] DNA-based catalysts,[7] amphiphilic copolymers,[8–10] star polymers,[11–15] micellar systems,[16–20] molecularly imprinted nano and microgels,[21–23] and dendrimers[24–28] were designed to achieve the necessary compartmentalization for efficient catalysis in water.

Supramolecular folding of polymer chains into single chain polymeric nanoparticles (SCPNs) is an attractive alternative to prepare compartmentalized, water-soluble, nanometer-sized particles with a hydrophobic interior.[29–32] Notably, the benzene-1,3,5-tricarboxamide (BTA) is an attractive unit to form SCPNs with well-defined, conformationally adaptable, three-dimensional structures as a result of the hydrogen-bond-driven, helical self-assembly of the BTA units.[31] Detailed scattering studies revealed that water-soluble copolymers based on oligo(ethylene glycol) methacrylate (*o*EGMA) and benzene-1,3,5-tricarboxamide methacrylate (BTAMA) fold in water into compact conformations

Additional Supporting Information may be found in the online version of this article.

© 2013 Wiley Periodicals, Inc.

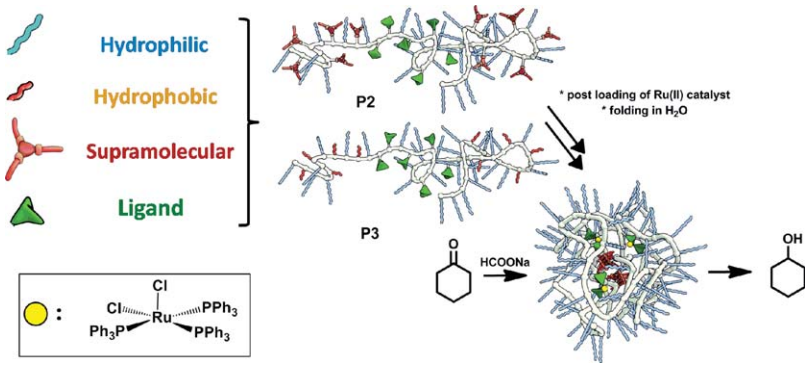

SCHEME 1 Design of catalytically active SCPNs for transfer hydrogenation of ketones in water.

consisting of a single polymer chain, and having a slightly elongated shape as a result of the BTA self-assembly.[29]

We recently inserted catalytically active moieties into BTA-based amphiphilic copolymers.[31,33] A set of random amphiphilic copolymers comprising *o*EGMA/BTAMA and L-proline units was prepared via reversible addition-fragmentation chain transfer (RAFT) polymerization.[33] The copolymers efficiently catalyzed aldol reactions with good diastereo- and enantioselectivities in water.[33] Remarkably, BTA self-assembly was crucial for effective catalysis in these copolymers, indicating that the creation of a stable but conformationally flexible hydrophobic interior into the SCPNs was crucial for catalysis to occur.[33]

In addition, Ru-catalyzed living free radical polymerization (LRP) was used to prepare a segmented amphiphilic *o*EGMA/BTAMA-based copolymer comprising diphenyl phosphinostyrene (SDP) units in the middle part, in which a ruthenium-based catalyst was simultaneously formed around the pendant SDP units via ligand exchange. The segmented copolymers formed SCPNs in water and catalyzed transfer hydrogenations of ketones.[31] In the Ru-based SCPNs, both the Ru-SDP complexation and the BTA stacking are elements that induce supramolecular folding of the polymer chain. Hence, it is intriguing to study in how far the BTA units are necessary as an additional structuring element for efficient catalysis, since this was so crucial in the L-proline-based organocatalytic system.[33]

Here we report our detailed investigations to understand in how far the directional, structuring role of BTA groups is important for the catalytic activity in transfer hydrogenation reactions catalyzed by Ru(II)-based SCPNs. We designed and synthesized a set of segmented, amphiphilic copolymers (Scheme 1) with a varying BTA content. The copolymers were synthesized via RAFT, an easy to apply, metal-free LRP technique, and then postloading of the Ru(II) catalyst was applied to create catalytic centers. Copolymers **P1–P5** were studied using spectroscopic techniques (circular dichroism and fluorescence spectroscopy) and dynamic light scattering (DLS) before and after Ru(II) loading. The activity of the copolymers was assessed in the transfer hydrogenation of cyclohexanone derivatives. The results show that BTA self-assembly is not required for the stabilization of the hydrophobic pocket when SDP-Ru complexes are present; hydrophobic monomers and SDP ligands effectively provide isolated, hydrophobic reaction pockets around ruthenium catalysts to induce efficient catalysis.

EXPERIMENTAL

Materials

Polymerizations, catalyst loadings and catalysis experiments were carried out by the syringe technique under dry argon in baked glass tubes equipped with a three-way stopcock. Poly (ethylene glycol) methyl ether methacrylate (PEGMA: $M_n \approx 475$) and lauryl methacrylate (LMA: Aldrich, purity >96%) were of commercial source (Aldrich), purified by an inhibitor removal column (Aldrich) and degassed by reduced pressure before use. The phosphine ligand monomer (diphenylphosphinostyrene: SDP), kindly supplied by Hokko Chemical (purity >99.9%), was degassed by reduced pressure before use. Azobisisobutyronitrile (AIBN) was recrystallized from methanol. 4-Cyano-4-methyl-5-(phenylthio)−5-thioxopentanoic acid was kindly provided by SyMO-Chem (Eindhoven, the Netherlands). Dioxane, dichloromethane, pentane and ethanol (Wako Chemicals, anhydrous; purity > 99%) were bubbled with dry nitrogen before use. 1,2,3,4-Tetrahydronaphthalene (tetralin; internal standard for ^{1}H NMR analysis) was dried over calcium chloride, distilled twice from calcium hydride and bubbled with dry nitrogen before use. $RuCl_2(PPh_3)_3$ (Aldrich, 97%) was used as received and handled in a glove box under a moisture- and oxygen-free argon atmosphere ($H_2O < 1$ ppm, $O_2 < 1$ ppm). Toluene (passed through purification columns; Solvent Dispensing System; Glass Contour) and hexane were bubbled with dry nitrogen for more than 15 min immediately before use. Sodium formate (Aldrich; purity > 98%) was used as received. Cyclohexanone, 4-methylcyclohexanone, 4-ethylcyclohexanone, 4-propylcyclohexanone (Aldrich, purity >99%), and H_2O (Wako; distilled) were of commercial source and bubbled with dry nitrogen for more than 15 min immediately before use. The synthesis of chiral BTAMA was performed as described elsewhere.[31] Nile Red was obtained from Sigma-Aldrich.

Characterization

The molecular weight M_n and M_w/M_n ratios of the polymers were measured by SEC in DMF containing 10 mM LiBr at 40 °C (flow rate = 1 mL/min) on three linear-type polystyrene

gel columns (Shodex KF-805L; exclusion limit = 4 × 10^6, pore size = 5000 Å, 0.8 cm i.d. × 30 cm) that were connected to a Jasco PU-2080 precision pump, a Jasco RI-2031 refractive index detector, and a Jasco UV-2075 UV–vis detector set at 270 nm. The columns were calibrated against 10 standard PMMA samples (Polymer Laboratories; M_n = 1680–1,200,000, M_w/M_n = 1.06–1.22) as well as MMA monomer. The absolute weight-averaged molecular weight (M_w) of polymers was determined by multi-angle laser light scattering (MALLS) in DMF containing 10 mM LiBr on a Dawn E instrument (Wyatt Technology: Ga-As laser; λ = 690 nm; scattering angle covered from 20° to 153°), in conjunction with the following SEC system: three linear-type polystyrene gel columns (shodex KF-805L; exclusion limit = 4 × 10^6; pore size = 5000 Å; particle size = 10 μm; 0.8 cm i.d. × 30 cm) connected to a Jasco PU-2080 precision pump, a Jasco RI-1530 refractive index detector, and a Jasco UV-1570 UV/vis detector set at 270 nm. The refractive index increment (dn/dc) was directly measured in DMF at 40 °C by the online RI-1530 refractive index detector. Fluorescence data were recorded on a Varian Cary Eclipse fluorescence spectrometer.

^{1}H NMR and ^{31}P NMR spectra were recorded at room temperature by a JEOL JNM-ECA500 spectrometer (operating at 500 MHz (^{1}H) and 202 MHz (^{31}P)). Proton chemical shifts are reported in ppm downfield from tetramethylsilane (TMS). Diethylphosphite $(C_2H_5O)_2P(O)H$ (12 ppm) was used as a standard for ^{31}P NMR.

Ultraviolet–visible (UV/Vis) and circular dichroism (CD) measurements were performed on a Jasco J-815 spectropolarimeter where the sensitivity, time constant and scan rate were chosen appropriately (sensitivity: standard; response: 2 s; band width: 1 nm; data pitch: 0.1 nm; scanning speed: 20 nm/min). Corresponding temperature-dependent measurements (data pitch: 0.1 °C) were performed with a PFD-425S/15 Peltier-type temperature controller with a temperature range of 263–383 K and adjustable temperature slope, in all cases temperature slope of 1 K/min was used. In all experiments the linear dichroism was also measured and in all cases no linear dichroism was observed. Separate UV/Vis spectra were obtained from a Perkin-Elmer UV/Vis spectrometer Lambda 40 (optical path length = 0.5 cm). The core-bound Ru(II) content was determined by inductively coupled plasma atomic emission spectroscopy (ICP-AES: CIROS^{CCD}; SPECTRO).

Dynamic light scattering measurements were performed on a Malvern μV Zetasizer equipped with an 830 nm laser. Samples were prepared by filtering solutions in MilliQ quality water through a 0.2 μm PVDF-filter (Whatman) in a fluorescence cell with a path length of 1 cm.

Synthesis

General Procedure for Polymerizations

CTA (12 mg, 0.043 mmol) and, for BTAMA containing copolymers, BTAMA (125 mg, 0.172 mmol (**P1**); 50 mg, 0.344 mmol (**P4**); 250 mg, 0.344 mmol (**P2**)) were placed in a 20 mL glass tube. Dioxane (6.5 mL) was added into the tube and the solution was stirred. *o*EGMA (1.7 mL, 3.75 mmol), for LMA containing polymers, LMA (0.12 mL, 0.42 mmol (**P5**, **P3**), 0.06 mL, 0.21 mmol (**P1**)) AIBN (4.2 mg, 0.026 mmol) and tetralin (0.1 mL) were added sequentially under dry argon at room temperature where the total volume of the polymerization mixture was 8.7 mL. Immediately after mixing, a small portion of the mixture was taken as a blank sample (t = 0) and the polymerization mixture was placed in an oil bath at 70 °C. For SDP containing polymers, SDP (0.35 mL of 730.839 mM in toluene, 0.256 mmol) was added under dry argon to the polymerization mixture after methacrylates reached around 30% conversion by ^{1}H NMR (1 h). Immediately after the addition of SDP monomer, the temperature was increased to 80 °C. The reaction was terminated after 8 h by cooling the mixture to room temperature (conv. *o*EGMA ≈ 90%; ^{1}H NMR). The monomer conversion was determined from the concentration of residual monomer measured by ^{1}H NMR with tetralin as an internal standard. The quenched reaction solutions were evaporated under vacuum and subsequently dissolved in DCM (1.5 mL) (**P3**, **P5**, **P6**) or for BTAMA containing polymers in MeOH/DCM (1/1, v/v, total 1.5 mL) (**P1**, **P2**, **P4**), and precipitated into cold hexane (11 mL) three times, evaporated to dryness and subsequently dried overnight under vacuum at room temperature.

oEGMA/BTAMA/LMA/SDP copolymer (P1)

^{1}H NMR (CD_2Cl_2): δ (ppm) = 8.40–8.29 (s, Ar-*H*: BTAMA), 7.83–7.77 (s, broad, N*H*CO), 7.62–7.31 (s, broad, Ar-*H*: SDP═O), 7.31–6.82 (s, broad, Ar-*H*: SDP), 4.13–3.89 (m, $CO_2CH_2CH_2$: oEGMA), 3.89–3.66 (m, $CO_2CH_2CH_2$: BTAMA, LMA), 3.66–3.43 (s, broad, OC_2H_4O), 3.37–3.22 (s, broad, —OCH_3), 2.00–1.48 (m, CH_2 backbone), 1.38–0.70 (m, broad, CCH_3 backbone, BTAMA and LMA pendants). SEC: M_n = 28,300, $Đ$ = 1.37.

oEGMA/BTAMA/SDP copolymer (P2)

^{1}H NMR (CD_2Cl_2): δ (ppm) = 8.40–8.29 (s, Ar-*H*: BTAMA), 7.83–7.77 (s, broad, N*H*CO), 7.62–7.31 (s, broad, Ar-*H*: SDP═O), 7.31–6.82 (s, broad, Ar-*H*: SDP), 4.13–3.89 (m, $CO_2CH_2CH_2$: oEGMA), 3.89–3.66 (m, $CO_2CH_2CH_2$: BTAMA), 3.66–3.43 (s, broad, OC_2H_4O), 3.37–3.22 (s, broad, —OCH_3), 2.00–1.48 (m, CH_2 backbone), 1.38–0.70 (m, broad, CCH_3 backbone, BTAMA pendant). SEC: M_n = 30,300, $Đ$ = 1.38.

oEGMA/LMA/SDP copolymer (P3)

^{1}H NMR (CD_2Cl_2): δ (ppm) = 7.62–7.31 (s, broad, Ar-*H*: SDP═O), 7.31–6.82 (s, broad, Ar-*H*: SDP), 4.01 (m, OCH_2CH_3), 4.13–3.89 (m, $CO_2CH_2CH_2$: oEGMA), 3.89–3.66 (m, $CO_2CH_2CH_2$: LMA), 3.66–3.43 (s, broad, OC_2H_4O), 3.37–3.22 (s, broad, —OCH_3), 2.00–1.45 (m, CH_2 backbone), 1.35–0.70 (m, broad, CCH_3 backbone, LMA pendant). SEC: M_n = 30,100, $Đ$ = 1.36.

oEGMA/LMA copolymer (P4)

^{1}H NMR (CH_2Cl_2): δ (ppm) = 4.13–3.89 (m, $CO_2CH_2CH_2$: oEGMA), 3.89–3.66 (m, $CO_2CH_2CH_2$: LMA), 3.66–3.43 (s, broad, OC_2H_4O), 3.37–3.22 (s, broad, —OCH_3), 2.00–1.45 (m,

TABLE 1 Characterization of Amphiphilic Copolymers[a]

Monomer Composition	DP_0 ($m/n/l/p$)[b]	M_n[c] (kDa)	$Đ$[c]	DP_{calcd} ($m/n/l/p$)[d]	$M_{n,calcd}$[e] (kDa)	M_w[f] (kDa)
(90%)-*o*EGMA/(5%)-BTA/(5%)-LMA/(**6%**) SDP (**P1**)	90/5/5/6	28.3	1.37	81/4.5/4.5/6	44.6	55.9
(90%)-*o*EGMA/(10%)-BTA/(**6%**)SDP (**P2**)	90/10/–/6	30.3	1.38	84.6/9.3/–/6	48.9	76.9
(90%)-*o*EGMA/(10%)-LMA/(**6%**)SDP (**P3**)	90/–/10/6	30.1	1.36	83.7/–/9.3/6	43.8	68.5
(90%)-*o*EGMA/(10%)-LMA (**P4**)	90/–/10/–	30.2	1.23	81.9/–/9/–	41.2	62.7
(90%)-*o*EGMA/(10%)-BTA (**P5**)	90/10/–/–	32.2	1.34	87/8/–/–	47.1	n.d.

[a] RAFT polymerization: ($[M_{tot}]_0/[CTA]_0/[AIBN]_0 = 530/5.2/2.5$ mM) ($[M_{tot}]$: $[oEGMA]_0 + [BTAMA]_0 + [LMA]_0 + [SDP]_0$) (P1–P5) in dioxane at 70 °C (increased to 80 °C after SDP addition).
[b] Degree of polymerization (DP_0): $m = [oEGMA]_0/[CTA]_0$; $n = [BTAMA]_0/[CTA]_0$; $l = [LMA]_0/[CTA]_0$; $p = [SDP]_0/[CTA]_0$.
[c] Analyzed by GPC in DMF (10 mM LiBr) with PMMA standard; $Đ = M_w/M_n$.
[d] DP_{calcd}: $m = [oEGMA]_0$ conv./$[CTA]_0$; $n = [BTAMA]_0 \times$ conv./$[CTA]_0$; $l = [LMA]_0$ conv./$[CTA]_0$; $p = [SDP]_0$ conv./$CTA]_0$. Conversion is determined by ^{1}H NMR in CD_3Cl at 25 °C.
[e] $M_{n,calcd} = F_{w,PEGMA} \times DP_{calcd,\ PEGMA} + F_{w,CTA1} + F_{w,BTAMA} \times DP_{calcd,BTA\text{-}MA} + F_{w,LMA} \times DP_{calcd,LMA} + F_{w,SDP} \times DP_{calcd,SDP}$.
[f] Analyzed by SEC-MALLS in DMF. n.d. = not determined.

CH_2 backbone), 1.45–0.70 (m, broad, CCH_3 backbone, LMA pendant). SEC: $M_n = 30{,}200$, $Đ = 1.23$.

General Procedure for Ruthenium Catalyst Loading

First, polymer and $RuCl_2(PPh_3)_3$ were solubilized in toluene-d_8 under argon, in separate tubes. Then, the Ru(II) solution was transferred via the syringe technique into the tube containing 1 mL polymer solution (2 mM in toluene-d_8) where the ratio was thus 2.5 equivalents of Ru(II) per polymer chain. The resulting mixture was stirred under argon at 80 °C for 12 h, and coordination of Ru(II) to the polymer SDP units was followed by ^{31}P and ^{1}H NMR. The polymer solution was concentrated *in vacuo* and precipitated into hexane under argon to remove triphenylphosphine liberated from Ru(II) catalyst. Then, the product was dried *in vacuo* at room temperature and the Ru(II) amount per a polymer gram was analyzed via ICP-AES: 53 μmol Ru/g for**P1**, 52 μmol Ru/g for **P2**, 54 μmol Ru/g for **P3**, 43 μmol Ru/g for **P4**, and 48 μmol Ru/g for **P5**.

General Procedure for Transfer Hydrogenations in Water

In a 10 mL glass tube, Ru(II)-bearing polymer (Ru = 0.001 mmol, polymer = 0.0004 mmol) and HCOONa (0.452 mmol, 30 mg) was placed and H_2O (1 mL) was added at 25 °C under argon. The solution was stirred at 80 °C for 5 min and the color change from brown to yellow was observed as an indicative of $Ru(II)H_2$ formation. After cooling, cyclohexanone (0.2 mmol, 0.020 mL) was immediately added into the solution ([Ru]/[cyclohexanone] = 1/200), and the mixture was placed in an oil bath at 40 °C. The conversion of the ketone was determined by ^{1}H NMR.

RESULTS AND DISCUSSION

Synthesis of Catalytically Active SCPNs

Amphiphilic copolymers (**P1–P5**) were synthesized by RAFT polymerization in dioxane at 70 °C in the presence of 4-cyano-4-methyl-5-(phenylthio)−5 thioxopentanoic acid as a chain transfer agent and AIBN as an initiator. We prepared copolymers with (**P1–P3**) and without (**P4–P5**) SDP ligands and copolymers with (**P1**, **P2**, **P5**) and without (**P3**, **P4**) BTA units. Lauryl methacrylate (LMA)—lacking structuring abilities—was chosen as a hydrophobic, nonhydrogen-bonding comonomer to replace BTAMA. To obtain SCPNs with comparable sizes and similar amphiphilic character, the theoretical degree of polymerization of methacrylates was kept constant ($DP_{th} = 100$) and the DP_{th}s for hydrophilic *o*EGMA and hydrophobic BTAMA and/or LMA were set as 90 and 10, respectively. For ligand-bearing copolymers (**P1–P3**), the SDP content was around 5.6 mol % of the total. The compositions of *o*EGMA, LMA and/or BTAMA are summarized in Table 1. To concentrate the SDP ligands in the middle of the polymer chain, SDP was directly added to the solution at around 30% conversion of methacrylates (after 1 h) for **P1–P3**. The reaction temperature was raised to 80 °C since styrene-based monomers require a higher polymerization temperature than methacrylates.

As an example, the results for the polymerization of BTAMA/LMA/*o*EGMA/SDP to afford **P1** are shown in Figure 1(a–c). The conversion of the monomers was quantified by the disappearance of the vinyl peaks via ^{1}H NMR [Fig. 1(a)]. After addition, SDP was rapidly consumed, followed by full conversion of the remaining methacrylates in 8 h. The molecular weights determined by SEC (relative to PMMA standards) increased with conversion [Fig. 1(b)] and the molecular mass distribution ($Đ$) remained narrow (<1.4) [Fig. 1(c)]. The almost identical consumption of the three different methacrylates together with the rapid consumption of SDP [Fig. 1(a)] indicates that a sequential, one-pot segmentation is achieved by the formation of two random end blocks of methacrylates and one middle random SDP/methacrylate block [Fig. 1(d)]. Copolymers **P2–P5** were obtained in a similar way using RAFT polymerization.

In our previous work, Ru(II)-loaded terpolymers were readily prepared via $RuCl_2(PPh_3)_3$-catalyzed LRP.[31] Efficient encapsulation of the polymerization catalyst resulted from

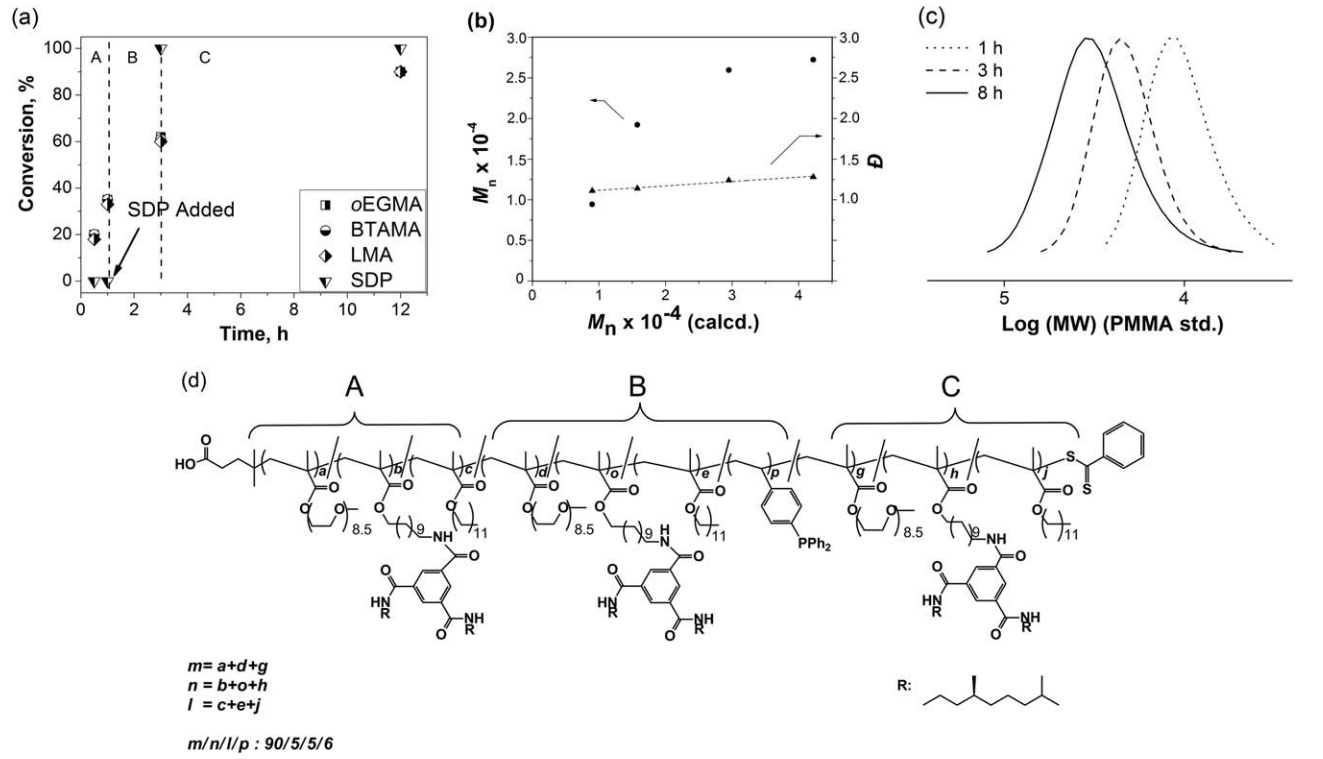

FIGURE 1 Synthesis of a segmented copolymer ligand (**P1**) by RAFT polymerization. (a) Conversion of monomers (*o*EGMA, BTAMA, LMA, and SDP) as a function of time, determined with ^{1}H-NMR; (b) number-average molecular weight (M_n) and molar mass distribution $Đ$ (M_w/M_n), determined by SEC (PMMA std) as a function of the number averaged molecular weights calculated from monomer conversion; (c) SEC curves of the samples obtained after 1, 3, and 8 h polymerization time; (d) chemical structure of **P1**. Conditions: $[o\text{EGMA}]_0/[\text{BTAMA}]_0/[\text{LMA}]_0/[\text{SDP}]_0/[\text{CTA}]_0/[\text{AIBN}]_0 = 478/27/27/32/5.2/2.5$ mM in dioxane at 70 °C (80 °C after SDP addition).

the exchange of ligands around the Ru(II) catalyst from PPh_3 units to SDP during the polymerization. As an alternative to this elegant, one-pot approach, we here apply a postencapsulation approach of the metal catalyst into the polymers to create catalytic centers, which permits control over the loaded amount of metal catalyst and ultimately, will permit to introduce various metal catalysts. Previously, the number of ruthenium atoms per chain was 2.5 (determined by ICP-AES), which is close to the maximum number of the available coordination sites (3) assuming that one ruthenium is at least supported by two SDP units.[31] To obtain an analogous system, an equivalent of 2.5 was applied for postloading of SCPNs in this work. Prior to the preparation of catalytically active SCPNs, we examined the coordination of $RuCl_2(PPh_3)_3$ (dichlorotris(triphenylphosphine) ruthenium(II) to **P3** by ^{1}H and ^{31}P NMR (Fig. 2, see Supporting Information Figure S1). **P3** exhibited a ^{31}P NMR signal at −1 ppm originating from the pendant SDP (Fig. 2). Upon catalyst loading, the SDP signal decreased due to Ru(II) coordination and a new signal appeared at 0.2 ppm. The signal at 0.2 ppm is attributed to free PPh_3, released from Ru(II) via the ligand exchange with **P3**-bound SDP. ^{1}H NMR showed broadening of the phenyl proton signals for polymer-bound SDP after Ru(II) loading owing to the low mobility, confirming the ligand exchange between SDP and PPh_3. No signal for free $RuCl_2(PPh_3)_3$ was observed around 50 ppm in all cases, implying quantitative immobilization of the fed Ru(II) cata-

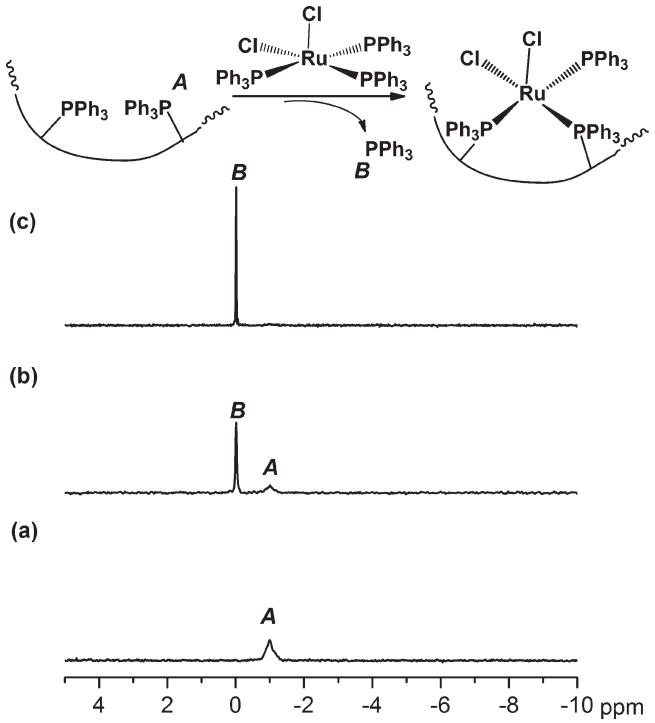

FIGURE 2 ^{31}P NMR spectra of polymer solutions (2 mM in toluene-d_8) 2.5 equivalents of Ru(II)) (a), 1 equivalent of Ru(II)) (b), and bare **P3** (c) in toluene-d_8 at r.t.

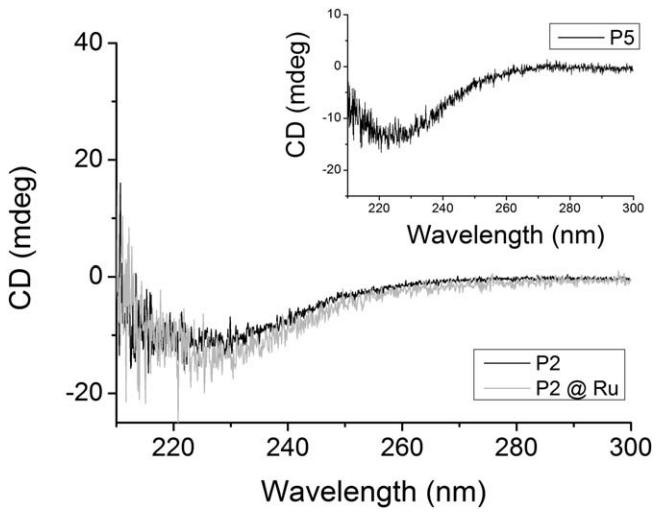

FIGURE 3 CD spectra of **P2**, **P2@Ru(II)**, and **P5** in H_2O ($c_{BTA} = 25$ μM at 313 K).

lyst. The same procedure was applied to other copolymers (**P1, P2, P4, P5**) and successful loading was confirmed by ICP-AES measurements (43–60 μmol Ru/g-polymer).

CD, DLS, and Fluorescence Characterization of P1–P5 in Solution

Circular dichroism (CD) spectroscopy is a powerfull technique to assess the presence of helical BTA-based aggregates within the SCPNs. We previously showed that a stereogenic center with an (*S*) configuration in the BTA side chain gives rise to a negative Cotton effect at $\lambda = 223$ nm, indicative of bias for the *M* helical sense.

Circular dichroism experiments were performed on **P1**, **P2**, and **P5** to evaluate the effect of SDP unit and Ru(II) catalysts on the helical self-assembly of the pendant BTA units before and after Ru(II) loading. The CD spectra of BTA-containing **P5**, SDP-containing **P2**, and Ru-bearing **P2** (Fig. 3, see Supporting Information Figure 5S for temperature-dependent CD spectra) showed a negative Cotton effect of around −15 mdeg. Since the magnitude of the Cotton effect is determined by the BTA concentration in BTA-based SCPNs,[31,33] the superimposable CD curves indicate that the SDP units do not affect the aggregation behavior of the pendant BTA units. Moreover, pseudo-crosslinking of the middle segment via the complexation of Ru(II) and the SDP ligands does not alter the magnitude of the Cotton effect, indicating that Ru(II)-SDP complexes do not significantly affect BTA aggregation. The sign and magnitude of the CD effect accord nicely with earlier observations.[31,34–38] These results suggest that the controlled topology of the polymer chains allows the self-assembly motifs, that is, BTA units and Ru(II)-SDP units, to act in an orthogonal way.[27,34]

Dynamic light scattering (DLS) experiments were performed to elucidate the single chain folding of the prepared copolymers. When linear polymers fold into SCPNs, hydrodynamic diameters (D_H) of around 10 nm are expected.[31] We here performed DLS studies of **P1–P5** before and after Ru(II) loading (Fig. 4); the values for D_H are summarized in Table 2. In all cases, we applied a polymer concentration of 18 mg mL^{-1}, identical to the concentrations used in the catalytic experiment (vide infra). The bare copolymers (**P1–P5**) show predominantly a single peak around 10 nm in DLS. The values for D_H vary between 7.5 and 11.7 nm (Table 2) and are in good correspondence to previously reported values. After Ru(II) loading, **P1–P3** kept a single chain character as evidenced by the presence of (predominantly) single peaks in Figure 4(c). Interestingly, for **P4** and **P5**—polymers that lack SDP ligands—large aggregates with sizes of 32–58 nm are observed after Ru(II) loading, indicative of multiple chain aggregation [Table 2, entries 4 and 5, Fig. 4(d)]. This is most probably caused by the Ru(II) catalyst that coordinates to available lone pairs of, for example, several BTA amides or *o*EG chains, thereby crosslinking a number of different polymer chains.

Finally, the presence of a hydrophobic interior in the SCPNs was evaluated with a solvatochromic dye, Nile Red. In pure water Nile Red displays low fluorescence intensity with an emission maximum of 660 nm. Decreasing the polarity of the medium results in an increase of the emission intensity and a shift of the emission maximum to lower wavelengths. This tool has been widely used to probe the formation of hydrophobic pockets within self-assembled structures.[39–41] The addition of copolymers (**P1–P5**) resulted in a blue shift of 27 nm for the emission wavelength of Nile Red in water. The fluorescence intensity also increased significantly in the presence of the polymers (Fig. 5). Both observations corroborate the presence of hydrophobic pockets in all polymer solutions. The solutions of polymers **P1**, **P2**, and **P5** with a BTA incorporation of 5, 10, and 10%, respectively, showed a stronger increase in fluorescence intensity compared to solutions of polymers **P3** and **P4**, which lack BTA units. This suggests that a more stabilized hydrophobic cavity upon incorporation of BTAs in a polymer can better accommodate Nile Red molecules compared to a polymer with LMA. In fact, judging from the intensity of fluorescence of polymers **P1–P5** that have identical DPs, the fluorescence intensity seems to be proportional to the BTA content of polymers **P1–P5**. This can be rationalized by the fact that the concentration of hydrophobic groups in BTA units is larger than in LMA units. Remarkably, polymer **P2** which has the same 10% BTA content as **P5**, displayed a much higher fluorescence intensity compared to **P5**. This is most probably due to the fact that further stabilization of the hydrophobic cavity is induced by the SDP units present in **P2**.

Transfer Hydrogenation of Cyclohexanone in Water

The catalytic activity of all copolymers was first evaluated in the transfer hydrogenation of cyclohexanone in water at 40°C ([substrate]/[HCOONa]/[Ru] = 0.2/0.5/0.001 M). From the conversions after 40 h, the turnover frequencies (TOF) were calculated; the results are summarized in Table 2. Ru(II)-bearing copolymers, **P1@Ru-P3@Ru**, showed TOF values of around 4.4 h^{-1}, indicating that the transfer

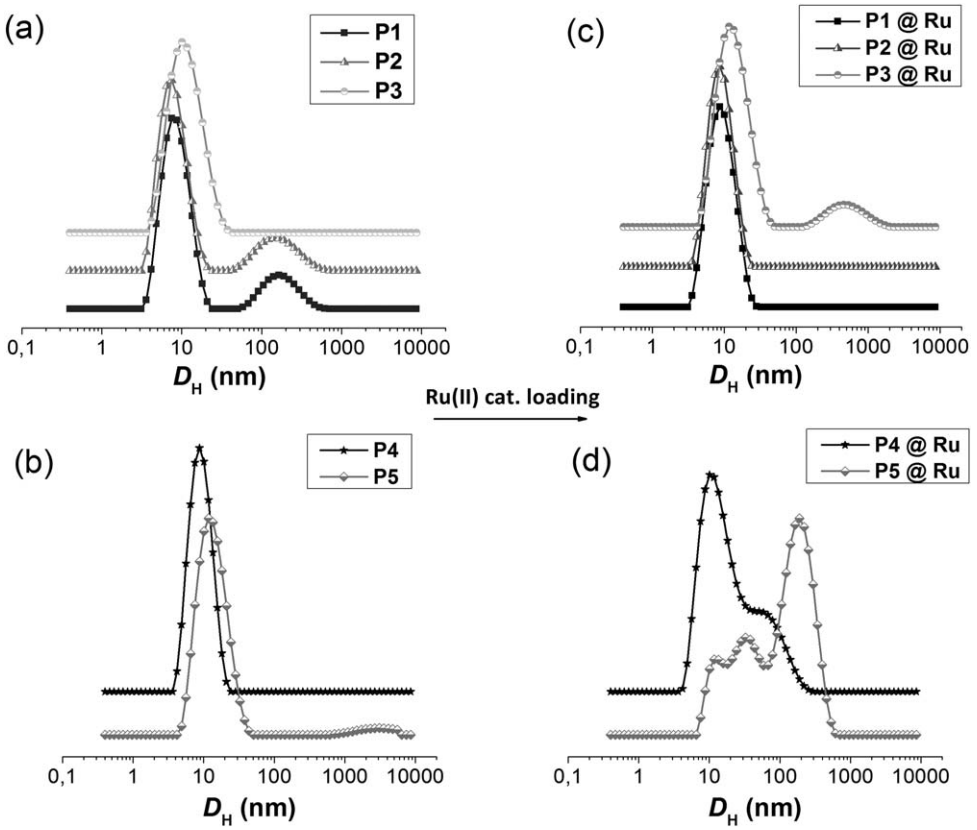

FIGURE 4 DLS intensity distribution for **P1–P5** before (a,b) and after (c,d) catalyst loading in H_2O at 40 °C, $c_{polymer} = 18$ mg mL^{-1}.

hydrogenations proceeded efficiently in the presence of SDP ligand and BTA or LMA hydrophobic units (Table 2, Entries 1–3). The values are smaller than those previously reported (TOF = 10–20 h^{-1}),[31] which is likely caused by the different method of Ru(II) incorporation. In addition, non SDP-bearing polymers with Ru(II), **P4@Ru** and **P5@Ru**, showed a TOF of 1.4 and 0 h^{-1}, respectively.

These results indicate that in the presence of SDP units, a further stabilization of the hydrophobic pocket via BTA self-assembly is not essential for catalytic activity. Almost no difference was observed in the activities between BTA-pendant polymers (**P1@Ru** and **P2@Ru**) and an LMA counterpart (**P3@Ru**) (Table 2, Entries 1–3). We propose that the pseudo-crosslinking of the SCPN by SDP- Ru(II) coordination sufficiently stabilizes the hydrophobic reaction spaces around the ruthenium complexes to shield and isolate the catalytic centers from the outer environments, thereby leading to efficient catalysis. Considering both the particle size distributions and TOF values with different polymers, it becomes clear that SDP-bearing SCPNs (**P1@Ru-P3@Ru** versus **P4@Ru**) lead to the highest catalytic activity. Non SDP-

TABLE 2 Hydrodynamic Radius (D_H) of **P1–P5** Before and After Ru(II) Complexation and Turnover Frequencies (TOF) Obtained in the Transfer Hydrogenation of Cyclohexanone

Entry	Code	D_H[a] (nm) (bare)	D_H[a] (nm) (Ru Loaded)	TOF[b] (h^{-1})
1	**P1**	10.0	8.7	4.4
2	**P2**	7.5	8.8	4.4
3	**P3**	8.7	11.6	4.3
4	**P4**	11.7	10.1; 58.8	1.4
5	**P5**	8.7	11.6; 32.6	0

(Ru/cyclohexanone/HCOONa): 0.001/0.2/0.5 M in H_2O at 40 °C.
[a] $c_{polymer} = 18$ mg/mL in H_2O at 40 °C.
[b] TOF = the amount of products (mol)\[the amount of the catalyst active sites × time (h)].

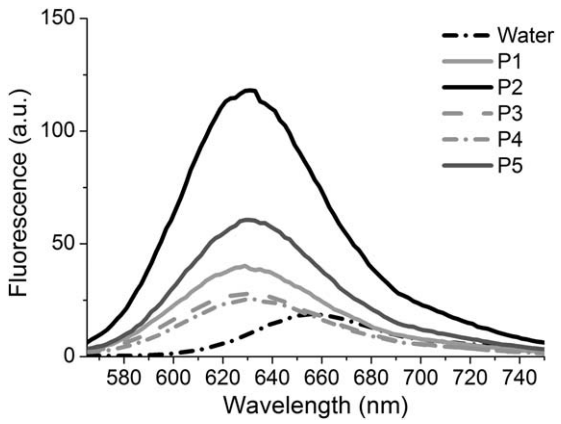

FIGURE 5 Fluorescence spectra of polymer/Nile Red solutions in water at 20 °C ($c_{Nile\ Red} = 5\ \mu M$, $c_{polymer} = 2\ \mu M$).

bearing polymers show aggregation of several chains after the addition of Ru(II), resulting in poor isolation of catalytic sites. This may result in undesired bimetallic interactions as a deactivating factor.[42]

More hydrophobic substrates, 4-methyl-, 4-ethyl-, and 4-propyl-cyclohexanone, were also subjected to transfer hydrogenation using **P3@Ru**. All of the substrates were efficiently converted into the corresponding alcohols with TOF values comparably to those of cyclohexanone (see Supporting Information Table 1S). This implies that designed catalytically active SCPNs were compatible with substrates of varying hydrophobicity.

CONCLUSIONS

We have shown a versatile way for the preparation of catalytically active SCPNs. A set of segmented copolymer ligands with a varying BTAMA content was obtained from RAFT polymerization. Postloading of ruthenium into the copolymers resulted in catalytically active SCPNs.

To understand the noncovalent, directional role of BTA units in the catalytic efficiency of SCPNs, the transfer hydrogenation of ketones in water was evaluated. The results showed that since the micro environment of the Ru catalyst is already tightly structured by metal-ligand coordination bonds, the structural elements of the remaining pocket is not decisive for catalytic performance as long as a hydrophobic pocket is maintained. Thus, in this particular system BTA stacking does not improve the catalytic activity or SCNP formation. Additionally, it was observed that immobilized Ru(II) by pendant SDP units is more efficient than "free" Ru(II) catalyst due to the efficient isolation of catalytic sites via single chain folding.

We expect that gaining a better insight into the essentials of a functioning hydrophobic cavity is a step forward to design compartmentalized systems that can perform tandem reactions as a result of the cooperative action of two or more catalytic cycles in one pot in water.

ACKNOWLEDGMENTS

This research was supported by The Netherlands Organization for Scientific Research (NWO) by an ECHO grant. They thank Mr. Yuta Koda (Kyoto University) for SEC-MALLS instruction; A. M. Elemans-Mehring for ICP-AES; and T.F.E. (Tim) Paffen for kindly providing **P5**. They acknowledge Hokko Chemical (Japan) for the kind supply of diphenylphosphinostyrene (SDP). The ICMS animation studio is acknowledged for providing the artwork.

REFERENCES AND NOTES

1 G. J. ten Brink, I.W. C. E. Arends, R. A. Sheldon, *Science* **2000**, *287*, 1636–1639.

2 K. H. Shaughnessy, *Chem. Rev.* **2009**, *109*, 643–710.

3 Z. Dong, Q. Luo, J. Liu, *Chem. Soc. Rev.* **2012**, *41*, 7890–7908.

4 M. Dürrenberger, T. Heinisch, Y. M. Wilson, T. Rossel, E. Nogueira, L. Knörr, A. Mutschler, K. Kersten, M. J. Zimbron, J. Pierron, T. Schirmer, T. R. Ward, *Angew. Chem. Int. Ed.* **2011**, *50*, 3026–3029.

5 J. Collot, J. Gradinaru, N. Humbert, M. Skander, A. Zocchi, T. R. Ward, *J. Am. Chem. Soc.* **2003**, *125*, 9030–9031.

6 M. T. Reetz, M. Rentzsch, A. Pletsch, M. Maywald, P. Maiwald, J. J.-P. Peyralans, A. Maichele, Y. Fu, N. Jiao, F. Hollmann, R. Mondiére, A. Taglieber, *Tetrahedron* **2007**, *63*, 6404–6414.

7 A. J. Boersma, J. E. Klijn, B. L. Feringa, G. Roelfes, *J. Am. Chem. Soc.* **2008**, *130*, 11783–11790.

8 B. M. Rossbach, K. Leopold, R. Weberskirch, *Angew. Chem.* **2006**, *118*, 1331–1335.

9 B. M. Rossbach, K. Leopold, R. Weberskirch, *Angew. Chem. Int. Ed.* **2006**, *45*, 1309–1312.

10 I. Okhapkin; E. Makhaeva; A. Khokhlov, In Conformation-Dependent Design of Sequences in Copolymers I; A. R. Khokhlov; Springer: Berlin, Heidelberg, **2006**; Vol. *195*, Chapter 3, pp 177–210.

11 A. W. Bosman, R. Vestberg, A. Heumann, J. M. J. Fréchet, C. J. Hawker, *J. Am. Chem. Soc.* **2003**, *125*, 715–728.

12 T. Terashima, M. Kamigaito, K.-Y. Baek, T. Ando, M. Sawamoto, *J. Am. Chem. Soc.* **2003**, *125*, 5288–5289.

13 T. Terashima, M. Ouchi, T. Ando, M. Sawamoto, *J. Polym. Sci. Part A: Polym. Chem.* **2010**, *48*, 373–379.

14 B. Helms, S. J. Guillaudeu, Y. Xie, M. McMurdo, C. J. Hawker, J. M. J. Fréchet, *Angew. Chem. Int. Ed.* **2005**, *44*,–384–6387.

15 Y. Chi, S. T. Scroggins, J. M. J. Fréchet, *J. Am. Chem. Soc.* **2008**, *130*, 6322–6323.

16 K. T. Kim, J. J. L. M. Cornelissen, R. J. M. Nolte, J. C. M. van Hest, *Adv. Mater.* **2009**, *21*, 2787–2791.

17 T.-H. Ku, M.-P. Chien, M. P. Thompson, R. S. Sinkovits, N. H. Olson, T. S. Baker, N. C. Gianneschi, *J. Am. Chem. Soc.* **2011**, *133*, 8392–8395.

18 A. D. Ievins, X. Wang, A. O. Moughton, J. Skey, R. K. O'Reilly, *Macromolecules* **2008**, *41*, 2998–3006.

19 A. C. Evans, A. Lu, C. Ondeck, D. A. Longbottom, R. K. O'Reilly, *Macromolecules* **2010**, *43*, 6374–6380.

20 P. Cotanda, A. Lu, J. P. Patterson, N. Petzetakis, R. K. O'Reilly, *Macromolecules* **2012**, *45*, 2377–2384.

21 S. Striegler, J. D. Barnett, N. A. Dunaway, *ACS Catal.* **2012**, *2*, 50–55.

22 Z. Chen, Z. Hua, J. Wang, Y. Guan, M. Zhao, Y. Li, *Appl. Catal. A* **2007**, *328*, 252–258.

23 G. Wulff, B.-O. Chong, U. Kolb, *Angew. Chem. Int. Ed.* **2006**, *45*, 2955–2958.

24 A. W. Bosman, H. M. Janssen, E. W. Meijer, *Chem. Rev.* **1999**, *99*, 1665–1688.

25 S. M. Grayson, J. M. J. Fréchet, *Chem. Rev.* **2001**, *101*, 3819–3868.

26 B. Helms, J. M. J. Fréchet, *Adv. Synth. Catal.* **2006**, *348*, 1125–1148.

27 B. Helms, E. W. Meijer, *Science* **2006**, *313*, 929–930.

28 J. Yu, T. V. RajanBabu, J. R. Parquette, *J. Am. Chem Soc* **2008**, *130*, 7845–7847.

29 M. A. J. Gillissen, T. Terashima, E. W. Meijer, A. R. A. Palmans, I. K. Voets, *Macromolecules* **2013**, *46*, 4120–4125.

30 E. A. Appel, J. Dyson, J. del Barrio, Z. Walsh, O. A. Scherman, *Angew. Chem. Int. Ed.* **2012**, *51*, 4185–4189.

31 T. Terashima, T. Mes, T. F. A. de Greef, M. A. J. Gillissen, P. Besenius, A. R. A. Palmans, E. W. Meijer, *J. Am. Chem. Soc.* **2011**, *133*, 4742–4745.

32 A. Sanchez-Sanchez, I. Pérez-Baena, J. Pomposo, *Molecules* **2013**, *18*, 3339–3355.

33 E. Huerta, P. J. M. Stals, E. W. Meijer, A. R. A. Palmans, *Angew. Chem. Int. Ed.* **2013**, *52*, 2978–2982.

34 T. Mes, R. van der Weegen, A. R. A. Palmans, E. W. Meijer, *Angew. Chem. Int. Ed.* **2011**, *50*, 5085–5089.

35 M. M. J. Smulders, I. A. W. Filot, J. M. A. Leenders, P. van der Schoot, A. R. A. Palmans, A. P. H.J. Schenning, E. W. Meijer, *J. Am. Chem. Soc.* **2010**, *132*, 611–619.

36 M. M. J. Smulders, M. M. L. Nieuwenhuizen, M. Grossman, I. A. W. Filot, C. C. Lee, T. F. A. de Greef, A. P. H. J. Schenning, A. R. A. Palmans, E. W. Meijer, *Macromolecules* **2011**, *44*, 6581–6587.

37 P. J. M. Stals, J. C. Everts, R. de Bruijn, I. A. W. Filot, M. M. J. Smulders, R. Martín-Rapun, E. A. Pidko, T. F. A. de Greef, A.R. A. Palmans, E. W. Meijer, *Chem. Eur. J.* **2009**, *16*, 810–821.

38 Y. Nakano, T. Hirose, P. J. M. Stals, E. W. Meijer, A. R. A. Palmans, *Chem. Sci.* **2012**, *3*, 148–155.

39 C. M. A. Leenders, L. Albertazzi, T. Mes, M. M. E. Koenigs, A.R. A. Palmans, E. W. Meijer, *Chem. Commun.* **2013**, *49*, 1963–1965.

40 C. B. Minkenberg, L. Florusse, R. Eelkema, G. J. M. Koper, J. H. van Esch, *J. Am. Chem. Soc.* **2009**, *131*, 11274–11275.

41 C. B. Minkenberg, F. Li, P. van Rijn, L. Florusse, J. Boekhoven, M. C. A. Stuart, G. J. M. Koper, R. Eelkema, J. H. van Esch, *Angew. Chem. Int. Ed.* **2011**, *50*, 3421–3424.

42 N. Madhavan, C. W. Jones, M. Weck, *Acc. Chem. Res.* **2008**, *41*, 1153–1165.